

Negative photoion spectroscopy of freon molecules in the vicinity of the Cl $2p$ edge

S. W. J. Scully, R. A. Mackie, R. Browning, K. F. Dunn, and C. J. Latimer

Department of Pure and Applied Physics, The Queen's University of Belfast, Belfast BT7 1NN, United Kingdom

(Received 11 February 2004; published 13 October 2004)

Polar photodissociation of $\text{CF}_n\text{Cl}_{4-n}$ ($n=0-2$) has been studied using synchrotron radiation within the energy range 195–217 eV. The first observations of negative photoion fragments from these molecules after core excitation are reported. In addition to observing a number of previously known resonances two additional resonant states, just above the Cl $2p$ ionization limit, are observed and play an important role in the polar photodissociation process. The difficulties in identifying these above threshold spin-split features using negative photoion spectroscopy are discussed.

DOI: 10.1103/PhysRevA.70.042707

PACS number(s): 33.80.Eh, 33.80.Gj

I. INTRODUCTION

Spectroscopy of core excited molecules is a valuable technique from which much information concerning symmetry and electronic structure can be obtained. Features observed in core excitation spectra are essentially characterized by resonances associated with the first empty molecular orbitals (MO's), which often appear as broad bands, as well as sharper structures involving transitions to Rydberg orbitals. The advantage of this technique as a means of investigating these unoccupied MO's lies in the simplicity of the interpretation of the spectral data due to the highly localized nature of the core electron.

Chlorine containing molecules such as carbon tetrachloride (CCl_4) and the freon molecules ($\text{CF}_n\text{Cl}_{4-n}$) are perfectly suited for inner shell spectroscopy using soft x-ray photons. In addition these molecules have received considerable attention due to the recognition that they are responsible for the depletion of the Earth's ozone layer through photochemical processes in the upper levels of the atmosphere [1,2]. In view of the importance of quantitative data for the photoexcitation of freons and CCl_4 , these molecules have been studied by a number of groups [3–11]. Much attention has also been given in electron impact studies to the inner shell transition regions involving the Cl $2p, 2s$ and C $1s$ electrons [12–23]. Schenk *et al.* [24] have reported photoion pair formation from freon molecules in the photon energy range 8–26 eV. They observed that the negative photoion yields of these halomethanes displayed similar patterns and that the monoatomic halogen negative ions (Cl^- and F^-) are dominant. To the best of our knowledge there have been no previously reported measurements concerning the polar photodissociation of CCl_4 .

In the valence-isoelectronic series of tetrahedral molecules, $\text{CF}_n\text{Cl}_{4-n}$ ($n=0-3$), only CCl_4 can have T_d symmetry. The electronic and vibrational spectra of tetrahedral molecules with T_d symmetry should in principle be relatively simple due to their high molecular symmetry. However, when these molecules are compared with the simpler tetrahedral methane (CH_4) molecule some differences arise. The C $1s$ x-ray absorption spectra of methane appears to be completely Rydberg like [15,25–27] showing no evidence of antibonding states. However CCl_4 seems to be dominated by

transitions to antibonding states with almost no evidence of Rydberg transitions [15]. The accepted model for molecules in which halogen atoms form a cage around the central carbon atom is that the diffuse Rydberg wave functions are expelled from within the cage [28]. The Rydberg states exist in an outer, shallower potential which has poor spatial overlap with the C $1s$ wave function. Whereas the antibonding states (which can also be regarded as scattering resonances for electrons trapped between the carbon atom and the ligands) have enhanced spatial overlap with the C $1s$ wave function. This effect is not observed in CH_4 because the H atoms have weaker scattering amplitude than the more electronegative halogens.

Although most previous measurements of polar photodissociation have been performed in the valence shell excitation region [29] a number of such studies have recently been reported in the core excitation energy range [30–33]. In the cases of CO and H_2O these investigations have shown that there is a complete suppression of shape resonance features. This is significant because shape resonances are a controversial subject in part because there is no generally agreed way to distinguish them unambiguously from doubly excited states [28]. However in our previous work involving the cage structured SF_6 molecule we have clearly observed the presence of shape resonances in the formation of fragment anions [34].

In the present work we have further investigated the role of antibonding and Rydberg states on cage type structures by studying negative photoion formation in CCl_4 and several freon molecules ($\text{CF}_n\text{Cl}_{4-n}$, $n=1, 2$) within the energy range 195–217 eV in the vicinity of the core Cl $2p$ energies.

II. EXPERIMENT

These experiments were performed at the Daresbury laboratory UK Synchrotron Radiation Source on beamline 5D, using a spherical grating monochromator which incorporates three gratings to provide photons within the energy range 20–215 eV. The experiments described here were carried out using the high energy grating (HEG) within the photon energy range 195–215 eV with a bandpass between 0.03 and 0.06 Å. Photons produced in the storage ring entered the experimental chamber via a 2.4 mm internal diameter glass

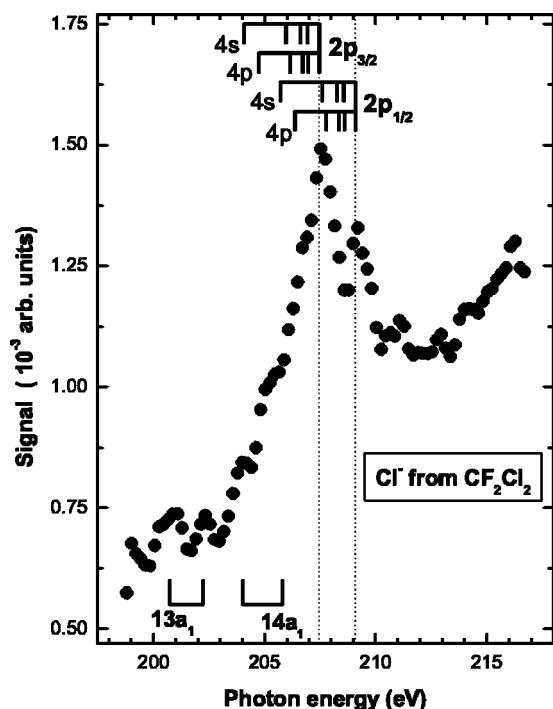


FIG. 1. Cl^- photoion yield curve obtained for CF_2Cl_2 in the vicinity of the $\text{Cl } 2p$ ionization edge. The vertical lines represent ionization potentials for the spin orbit split $\text{Cl } 2p$ electrons. Also marked are Rydberg states converging onto these ionization limits ($2P_{1/2}np$, $2P_{1/2}ns$, $2P_{3/2}np$, $2P_{3/2}ns$) and unoccupied valence orbitals associated with $\text{Cl } 2p$ excitation.

capillary, were crossed at 90° by a low pressure gas jet of the target species and subsequently detected using an Al_2O_3 photocathode. The photon flux was obtained by taking into account the relative detection efficiency of the photocathode with respect to wavelength [35].

A triple-quadrupole mass spectrometer (Hiden Analytical HAL IV IDP) was then used to analyze the negative ion fragments produced in polar photodissociation of the target species. The ions formed in the interaction region were swept towards the quadrupole by an electrostatic field, ~ 10 V/cm, defined by a pair of high transparency mesh grids. Negative ions with a stable trajectory within the triple-quadrupole mass spectrometer were detected by an off-axis channel electron multiplier. The data presented here have been normalized to account for target gas density by calibrating the sensitivity of the ionization gauge to within $\pm 7\%$ for the different species investigated, using an MKS Baratron type 170 capacitance manometer. The photon energy was calibrated by comparing the positive ion yield produced after $S 2p$ core electron excitation of SF_6 with the high resolution photoabsorption spectrum measured by Hudson *et al.* [36].

III. RESULTS

A. CF_2Cl_2

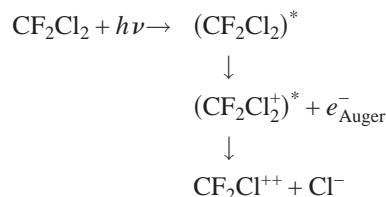
The ground state electronic configuration of CF_2Cl_2 (in C_{2v} symmetry) is given by

$$(1b_2^2 1a_1^2)(2a_1^2 1b_1^2)(3a_1^2) \\ (2b_2^2 4a_1^2)(5a_1^2 3b_2^2 4b_2^2 2b_1^2 1a_2^2 6a_1^2) \\ (7a_1^2 3b_1^2 8a_1^2 5b_2^2 9a_2^2 6b_2^2 10a_1^2 4b_1^2 11a_1^2 2a_2^2 5b_1^2 7b_2^2 12a_1^2 3a_2^2 6b_1^2 8b_2^2),$$

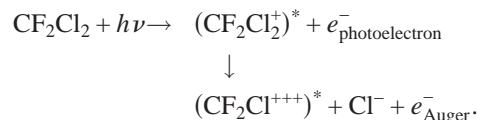
where the parentheses denote the $\text{Cl } 1s$, $\text{F } 1s$, $\text{C } 1s$, $\text{Cl } 2s$, $\text{Cl } 2p$, and valence orbitals respectively. In addition there are unoccupied valence antibonding orbitals $13a_1^0$, $9b_2^0$, $7b_1^0$, and $14a_1^0$ which have $(\text{C-Cl})^*$, $(\text{C-Cl})^*$, $(\text{C-F})^*$, and $(\text{C-F})^*$ character, respectively.

Figure 1 shows the first measurements of the Cl^- yield curve in the energy region required for $\text{Cl } 2p$ excitation (195–217 eV). This ion yield curve was obtained with a photon energy resolution of 0.06 \AA (200 meV at 205 eV). A small F^- signal was obtained at these energies however no resonant structure was observed. $\text{Cl } 2p$ inner shell excitation studies of CF_2Cl_2 have been made by several groups using electron energy loss techniques [15], photoabsorption techniques [37] and photoion-photoion coincidence (PIPICO) techniques [19]. The assignments used to describe some of the resonant structure observed in the Cl^- yield are given in Table I and follow those of Zhang *et al.* [15]. The intensity distributions of the $\text{Cl } 2p_{3/2}13a_1$, $14a_1$ and $\text{Cl } 2p_{1/2}13a_1$ transitions are slightly different to those observed in the photoabsorption measurements.

The formation of Cl^- after $\text{Cl } 2p$ electron excitation may follow a spectator Auger decay mechanism similar to that observed in SO_2 [38] and SF_6 [34]. Cl^- was not observed after $\text{Cl } 2p$ excitation in CF_3Cl , which is suggestive of the fact that the atom which has the core hole or vacancy after photoabsorption is not involved in the negative ion channel. If spectator Auger decay is responsible for the negative ion fragmentation at these high energies then a process such as



may occur. Indeed above the $\text{Cl } 2p$ ionization potentials, where a large negative ion continuum is observed, the process may be



In both cases the multiply charged fragment can undergo further dissociation. The negative ion continuum appears to be a function of photon energy, which is probably a result of the negative ion no longer being produced from a resonant state and the ejected core electron can now carry away any excess energy. The chlorine anion may also be formed via ultrafast dissociation which occurs before Auger decay. Anion production via ultra-fast dissociation has recently been observed in $\text{Br}(\text{CH}_2)_n\text{Cl}$ [39].

TABLE I. Experimental energies for resonances in the Cl^- spectra obtained from CF_2Cl_2 . The uncertainty in the term values for the above threshold resonances arises from the quadrature sum of the 40 meV uncertainty in the energy of the Cl $2p$ ionization potentials and the 150 meV uncertainty of the resonance position.

Energy ± 0.15 (eV)	Term value (eV)	Electronic transition
200.73	6.74	$2p_{3/2} \rightarrow 13a_1$
202.23	6.87	$2p_{1/2} \rightarrow 13a_1$
204.04	3.43	$2p_{3/2} \rightarrow 14a_1$
204.07	3.24	$2p_{3/2} \rightarrow 4s$
205.70	3.40	$2p_{1/2} \rightarrow 4s$
205.80	3.30	$2p_{1/2} \rightarrow 14a_1$
207.47		$(2p_{3/2})^{-1}$
207.53	-0.06 ± 0.16	$2p_{3/2} \rightarrow \sigma^*$ or $2e^-$
209.10		$(2p_{1/2})^{-1}$
209.20	-0.10 ± 0.16	$2p_{1/2} \rightarrow \sigma^*$ or $2e^-$

Some of the below threshold resonant features have been assigned to photoexcitation into antibonding unoccupied valence orbitals, $13a_1$, $9b_2$, $14a_1$, and $7b_1$. This excitation will only be intense if the antibonding orbital is spatially close to the originating orbital [40]. Additionally, mixing between the antibonding and Rydberg orbitals of the same symmetry should be small. Extensive mixing of unoccupied valence and Rydberg orbitals will distribute the oscillator strength between many excitations resulting in a broad rather than a single distinct transition. In the case of a molecule which has a potential barrier, penetration of the diffuse Rydberg orbitals into the inner molecular region is avoided and the antibonding orbitals may behave as quasibound states. The first few peaks at 200.73 eV and 202.23 eV appear to be well separated from any possible Rydberg states and are believed to be purely due to excitation into unoccupied valence orbitals. However the features at higher energies may have contributions from both Rydberg and unoccupied valence orbitals. Rydberg states converging onto the ionization limits of the Cl $2p$ electrons are marked on Fig. 1. They have been identified using the previously reported quantum defects of King and McConkey [41]. The most intense features, which appear to reach their respective maxima at ≈ 0.1 eV above the Cl $2p$ ionization potentials, are due to previously unobserved states. These two peaks have been fitted to Voigt functions, i.e., by a Lorentzian function convoluted with a Gaussian function. The Lorentzian width should give a measure of the width of the state, whereas the Gaussian width corresponds to the instrumental broadening due to the resolution of the monochromator. These fits give linewidths of 2.2 ± 0.4 eV ($2p_{3/2}$) and 0.7 ± 0.5 eV ($2p_{1/2}$). The fact that all of these resonant states are only observed in the Cl^- channel suggests, if the spectator Auger decay mechanism holds, that they are all to some extent localized in the vicinity of the Cl atoms. This localization could explain why no resonant structure is observed in the F^- channel. The absence of resonant structure in the Cl^- channel after Cl $2p$ excitation in CF_3Cl also suggests that the ligand with the core hole cannot undergo decay to become a negative ion. This is notably

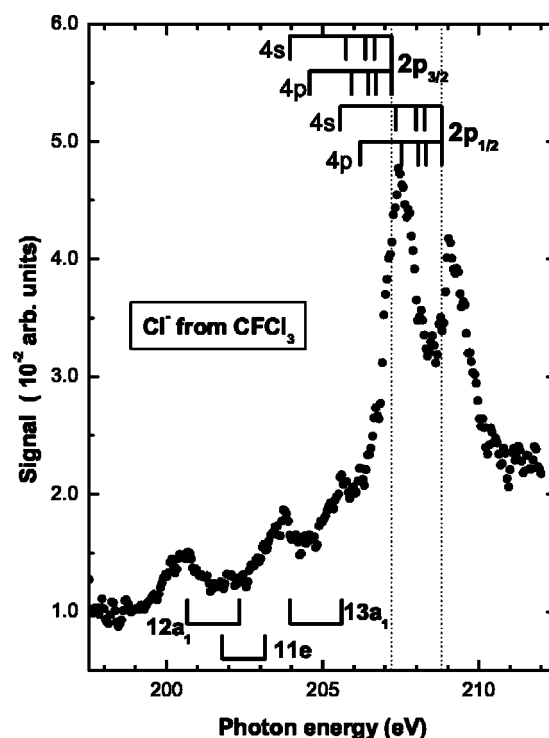


FIG. 2. Cl^- photoion yield curve obtained for CFCl_3 in the vicinity of the Cl $2p$ ionization edge. The vertical lines represent ionization potentials for the spin orbit split Cl $2p$ electrons. Also marked are Rydberg states converging onto these ionization limits ($2P_{1/2} \rightarrow np$, $2P_{1/2} \rightarrow ns$, $2P_{3/2} \rightarrow np$, $2P_{3/2} \rightarrow ns$) and unoccupied valence orbitals associated with Cl $2p$ excitation.

different to what was observed in SF_6 where S^- was observed after S $2p$ excitation [34].

B. CFCl_3

The ground state electronic configuration of CFCl_3 (in C_{3v} symmetry) is given by

$$(1a_1^4 1e^4)(2a_1^2)(3a_1^2)(2e^4 4a_1^2)(5a_1^2 3e^4 1a_2^2 4e^4 6a_1^2 5e^4) \\ (7a_1^2 8a_1^2 6e^4 9a_1^2 10a_1^2 7e^4 8e^4 11a_1^2 9e^4 10e^4 2a_2^2) \\ {}^1A_1,$$

where the parentheses denote the Cl $1s$, F $1s$, C $1s$, Cl $2s$, Cl $2p$, and valence orbitals respectively [15]. In addition there are unoccupied valence antibonding orbitals $12a_1^0$, $11e^0$, and $13a_1^0$ which have $(\text{C-Cl})^*$, $(\text{C-Cl})^*$, and $(\text{C-F})^*$ character, respectively. Figure 2 shows the Cl^- ion yield curve obtained after photoexcitation of the Cl $2p$ inner shell electrons of CFCl_3 . The Cl^- yield was measured with a photon energy resolution of 0.03 \AA (100 meV at 205 eV).

Spectroscopic measurements for Cl $2p$ electrons in CFCl_3 have been performed previously by groups using electron energy loss techniques [15,42], photoion mass spectrometry [20] and photoion-photoion coincidence techniques [19]. The assignments of Zhang *et al.* [15] have been used to describe

TABLE II. Experimental energies for resonances in the Cl⁻ spectra obtained from CFCl₃.

Energy ±0.15(eV)	Term value (eV)	Electronic transition
200.65	6.55	$2p_{3/2} \rightarrow 12a_1$
201.79	5.41	$2p_{3/2} \rightarrow 11e$
202.33	6.50	$2p_{1/2} \rightarrow 12a_1$
203.15	5.66	$2p_{1/2} \rightarrow 11e$
203.96	3.24	$2p_{3/2} \rightarrow 4s, 13a_1$
205.57	3.24	$2p_{1/2} \rightarrow 4s$
205.62	3.19	$2p_{1/2} \rightarrow 13a_1$
207.20		$(2p_{3/2})^{-1}$
207.43	-0.23±0.16	$2p_{3/2} \rightarrow \sigma^*$ or $2e^-$
208.81		$(2p_{1/2})^{-1}$
209.03	-0.22±0.16	$2p_{1/2} \rightarrow \sigma^*$ or $2e^-$

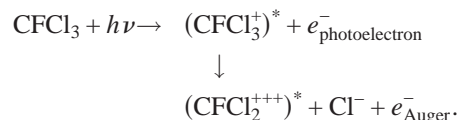
the below threshold resonances observed in the Cl⁻ yield curve shown in Fig. 2. The present assignments and their experimental energies are listed in Table II.

The Cl⁻ yield observed in the vicinity of the Cl $2p$ edge has a maximum which is nearly a factor of 30 times the size of the largest Cl⁻ signal obtained after Cl $2p$ excitation in CF₂Cl₂. This large increase cannot be explained using the simple idea of having an extra chlorine ligand in this molecule. Zhang *et al.* [15] have observed a slight increase in the oscillator strength for CFCl₃ compared to CF₂Cl₂ in the energy region required for Cl $2p$ excitation, however it is not as large an increase as that observed in the negative ion channel. In fact the increases in photoabsorption oscillator strength at the Cl $2p$ edge as we progress along the CF₃Cl to CCl₄ chain appear to be proportional to the number of Cl ligands. This does not appear to be the case in this study of the Cl⁻ fragments.

It is thought that the Cl⁻ photoion production resulting from inner shell excitation of CFCl₃ is due to spectator Auger decay in a similar manner to that described for the CF₂Cl₂ molecule. Again we see contributions from unoccupied valence and Rydberg orbitals below the Cl $2p$ ionization thresholds, and from previously unobserved resonance states just above the ionization thresholds. The term values for the unoccupied valence orbitals appear to be slightly smaller than the corresponding term values observed in CF₂Cl₂, whereas the term values for the above threshold states appear to be slightly larger.

The Voigt profiles fitted to these two peaks give linewidth values of 0.98 ± 0.10 eV ($2p_{3/2}$) and 0.83 ± 0.15 eV ($2p_{1/2}$). There appears to be structure with a spacing of 0.4 eV on top of the resonances which may be due to vibrational levels or it may be due to two electron excitation processes occurring in the same energy region, similar to that observed for SF₆ after S $2p$ excitation [34]. The mixing of Rydberg orbitals with unoccupied valence orbitals appears more clearly in CFCl₃ than in the CF₂Cl₂. Two sharp features at 204 and 205.5 eV superimposed on top of broader features appear to agree well with the assignment of $4s$ Rydberg orbitals converging onto the spin orbit split Cl $2p$ ionization potentials. Here again the Rydberg states were obtained us-

ing the quantum defects of King and McConkey [41]. The broader features appear to be due to the antibonding $13a_1$ (C-F)* and $11e$ (C-Cl)* unoccupied valence orbitals. Interestingly the intensity distribution of these unoccupied valence orbitals agrees well with that observed in the electron energy loss work of Zhang *et al.* [15]. The negative ion yield curve above the Cl $2p$ ionization thresholds is considerably larger than the yield below the inner core transitions. Similar behaviour was observed in CF₂Cl₂ and it is thought that it is due to polar photodissociation from an excited ionic state, such that



Here spectator Auger decay no longer occurs because the excited electron is now in the continuum. It is also no longer a resonant process since the ejected electron can remove excess energy and a continuum of negative ion signal is obtained.

C. CCl₄

The ground state configuration of CCl₄ (in T_d symmetry) is given by

$$\begin{aligned} (1t_2^6 1a_1^2)(2a_1^2)(2t_2^6 3a_1^2)(3t_2^6 4a_1^2 1t_1^6 1e^4 4t_2^6) \\ (5a_1^2 5t_2^6 6a_1^2 6t_2^6 2e^4 7t_2^6 2t_1^6) \\ {}^1A_1, \end{aligned}$$

where the parentheses denote the Cl $1s$, C $1s$, Cl $2s$, Cl $2p$, and valence orbitals, respectively [15]. In addition there are unoccupied valence antibonding orbitals $7a_1^0$ and $8t_2^0$ which both have (C-Cl)* character. The analysis for CCl₄ to date has been based on T_d symmetry, however, the isotopic distribution of Cl (75.5% Cl³⁵, 24.5% Cl³⁷) breaks the symmetry of the molecule so that it consists of a mixture of five isotopomers; two of T_d , two of C_{3v} , and one of C_{2v} symmetry [18].

The Cl⁻ photoion yield curve obtained for CCl₄ in the vicinity of the Cl $2p$ ionization edge is shown in Fig. 3. This yield curve was measured with a photon energy resolution of 0.03 Å (100 meV at 205 eV). Much previous work has been carried out on the Cl $2p$ photoexcitation processes in CCl₄, including electron energy loss [12,15,16,42] and photoabsorption [17,18,37] spectroscopies. The abundance of earlier spectroscopic studies allows for a relatively easy interpretation of the below edge resonances observed in the Cl⁻ yield curve. These assignments are shown in Fig. 3 and tabulated in Table III. According to their large term values the 200.31 and 201.85 eV bands are assigned as transitions to the C-Cl antibonding orbital $7a_1$ from the Cl $2p_{3/2}$ and Cl $2p_{1/2}$ orbitals, respectively. The $8t_2$ orbital appears to have 4 bands associated with it and Ho [17] has suggested that this is due to Jahn-Teller components of the transitions from the spin orbit split Cl $2p$ orbitals. However de Simone *et al.* [18] have also suggested that the fact that CCl₄ is made up of five isotopomers may produce the splitting. The progressive low-

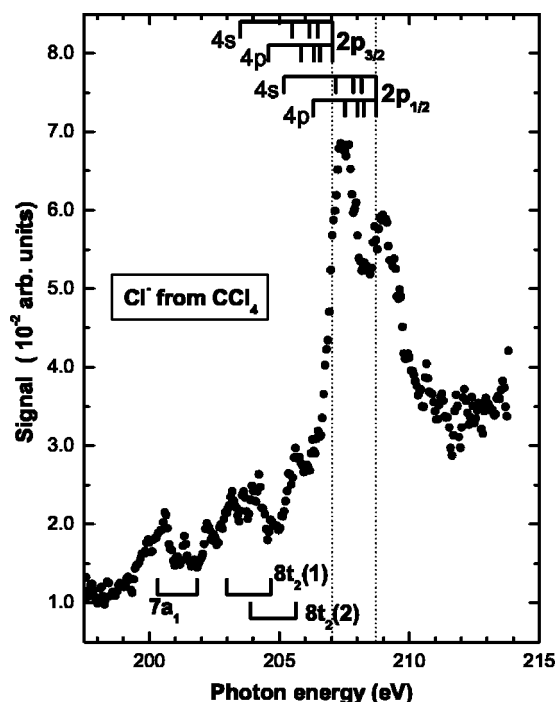


FIG. 3. Cl^- photoion yield curve obtained for CCl_4 in the vicinity of the Cl $2p$ ionization edge. The vertical lines represent ionization potentials for the spin orbit split Cl $2p$ electrons. Also marked are Rydberg states converging onto these ionization limits ($2P_{1/2} \rightarrow np$, $2P_{1/2} \rightarrow ns$, $2P_{3/2} \rightarrow np$, $2P_{3/2} \rightarrow ns$) and unoccupied valence orbitals associated with Cl $2p$ excitation.

ering of symmetry may split the t_2 state into two and then three dipole allowed substates.

The present data shows fine structure not observed in previous methods even though the resolution used is of the same order, if not worse, than the previous measurements. The fact that this structure is observed more in the second broad peak than in the first suggests that it is due to Rydberg states converging onto the Cl $2p$ edges. These Rydberg states may be too weak to be observed in photoabsorption, but may actually provide quite strong channels when the photoion pair process is considered.

The two most intense resonance peaks that occur ≈ 0.37 eV above their respective ionization thresholds have also been observed by de Simone *et al.* [18] and Ho [17] in their photoabsorption spectra. de Simone *et al.* measured the energies at the center of each peak to be 207.36 and 209.03 eV in agreement with the present data. Their measured widths for these states, which were both 1.33 eV, are in reasonable agreement with the linewidths obtained from the present data. The linewidths obtained from Voigt profiles are 0.95 ± 0.15 eV ($2p_{3/2}$) and 1.34 ± 0.15 eV ($2p_{1/2}$). de Simone *et al.* attributed these peaks to quasibound σ^* (shape) resonances. Whereas Ho proposed that they originated from two-electron excitation or shape resonance.

The peak at 207.41 eV is only a factor of 1.4 larger than the comparable shape resonance state in CFCl_3 . This is very different to the much larger change that is seen going from CF_2Cl_2 to CFCl_3 . Zhang *et al.* [15] compared the oscillator strength per Cl atom for Cl $2p$ excitations of

TABLE III. Experimental energies for resonances in the Cl^- spectra obtained from CCl_4 .

Energy ± 0.15 (eV)	Term value (eV)	Electronic transition
200.31	6.73	$2p_{3/2} \rightarrow 7a_1$
201.85	6.88	$2p_{1/2} \rightarrow 7a_1$
202.98	4.06	$2p_{3/2} \rightarrow 8t_2(1)$
203.50	3.54	$2p_{3/2} \rightarrow 4s$
203.89	3.15	$2p_{3/2} \rightarrow 8t_2(2)$
204.67	4.06	$2p_{1/2} \rightarrow 8t_2(1)$
205.19	3.54	$2p_{1/2} \rightarrow 4s$
205.64	3.09	$2p_{1/2} \rightarrow 8t_2(2)$
207.04		$(2p_{3/2})^{-1}$
207.41	-0.37 ± 0.16	$2p_{3/2} \rightarrow \sigma^*$ or $2e^-$
208.73		$(2p_{1/2})^{-1}$
209.09	-0.36 ± 0.16	$2p_{1/2} \rightarrow \sigma^*$ or $2e^-$

CF_3Cl , CF_2Cl_2 , CFCl_3 , and CCl_4 , and found that all of these curves had approximately the same peak in oscillator strength with a value per Cl atom of $\approx 3.65 \times 10^{-2} \text{ eV}^{-1}$. This implies that the oscillator strength increases linearly with increasing number of Cl ligands. The ratio between the CFCl_3 and CCl_4 oscillator strengths after Cl $2p$ excitation should therefore be 4/3, which is very similar to the increase we observe in the Cl^- signal between CFCl_3 and CCl_4 . However this additivity rule is clearly not in accord with the change observed between the CF_2Cl_2 to CFCl_3 and it is not clear what causes this. It is suspected that symmetry considerations and bond lengths may play a role in the Cl^- formation. This could produce the anomalous behavior observed especially since it appears likely that the negative ion formation is sensitive to the localization of the excited electron. The lack of any resonant structure in the F^- yield after Cl $2p$ excitation provides evidence for such a localization effect.

IV. DISCUSSION

The origin, and term values, of the two dominant resonant features observed for the first time in the freon molecules studied in the present work, remains a difficult question. The equivalent features have been observed previously in CCl_4 photoabsorption cross sections and thus attributed to either shape resonances or two electron excitation by different workers [17,18]. In our earlier work [34] we have shown that in SF_6 , which has a similar cage-like structure to CCl_4 and is considered to provide prototype examples of shape resonance phenomena, such resonances can have lifetimes in the femtosecond regime—long enough for a trapped electron to behave as a spectator while Auger decay takes place.

In the present work, as the molecule was progressively changed from CCl_4 to CF_2Cl_2 , the term values of these quasibound resonant states is found to decrease. These changes in term values are most likely related to changes in the C-Cl bond length. According to Pauling [43] attaching a fluorine atom to the same carbon atom as a chlorine atom will produce shortening of the C-Cl bond—a result of partial double

bond formation with some of the carbon bond orbital being released by the large ionic character of the C-F bond. It is to be expected therefore that, as further fluorine atoms are substituted into the freon molecules, the C-Cl bond lengths will further decrease and this effect is seen in the *ab initio* calculations of Shimizu *et al.* [44] for CF₃Cl, CF₂Cl₂, and CFC1₃. In addition Zhang *et al.* [15] have shown that the term value of the ($1s \rightarrow t_2$) transition in CCl₄ is larger than in CF₄ which illustrates that the inner well potential of CCl₄ is stronger. This is also consistent with the C-Cl bond length being greater than the C-F. Therefore we might expect the term value of any shape resonance state to increase as more chlorine ligands are substituted onto the carbon atom—in accord with what we observe in the present work. However it should be noted that the relationship between bond length and shape resonance energy position is a controversial topic in the literature. One school of thought is doubtful about any clear well defined connection while the other is actually prepared to assume a linear relationship and use it to derive bond distances in absorbed molecules. The situation has most recently been discussed in detail in a review by Piancastelli [28] and in it she concludes that any correlation between bond length and shape resonance is not a reliable way to assign such features.

The alternative assignment, namely that the features we observe are due to two electron excitation processes is also not without problems—most noticeably the fact that such excitations are not normally found to have a larger oscillation strength than single electron excitation. Although two electron excitations have been seen using anion yield spectroscopy in CO and H₂O [30,32,33] where the shape resonance channel was suppressed, these excitations were substantially smaller than the one electron Rydberg and molecular orbital excitations, unlike the features observed in the present work. It is of course quite possible that both types of excitation are occurring as we have observed previously in SF₆ [34].

ACKNOWLEDGMENTS

The authors would like to thank the staff of the Daresbury Laboratory UK Synchrotron Radiation Source for their assistance. The support of the UK Engineering and Physical Science Research Council in providing a research grant is also gratefully acknowledged. One of us (S.W.J.S.) was the recipient of support from the Department of Education, Northern Ireland.

-
- [1] H. I. Schiff, *Nature (London)* **305**, 471 (1983).
 [2] D. J. Wuebbles, *J. Geophys. Res., C: Oceans Atmos.* **88**, 1433 (1983).
 [3] W. Zhang, G. Cooper, T. Ibuki, and C. E. Brion, *Chem. Phys.* **151**, 343 (1991).
 [4] W. Zhang, G. Cooper, T. Ibuki, and C. E. Brion, *Chem. Phys.* **151**, 357 (1991).
 [5] W. Zhang, G. Cooper, T. Ibuki, and C. E. Brion, *Chem. Phys.* **153**, 491 (1991).
 [6] J. W. Au, G. R. Burton, and C. E. Brion, *Chem. Phys.* **221**, 151 (1997).
 [7] J. Doucet, P. Sauvageau, and C. Sandorfy, *J. Chem. Phys.* **58**, 3708 (1973).
 [8] T. Cvitas, H. Gusten, and L. Klasnic, *J. Chem. Phys.* **67**, 2687 (1977).
 [9] A. W. Potts, F. Quinn, G. V. Marr, B. Dobson, I. H. Hillier, and J. B. West, *J. Phys. B* **18**, 3177 (1985).
 [10] G. M. Bancroft, J. D. Bozek, J. N. Cutler, and K. H. Tan, *J. Electron Spectrosc. Relat. Phenom.* **47**, 187 (1988).
 [11] J. D. Bozek, G. M. Bancroft, J. N. Cutler, K. H. Tan, and B. W. Yates, *Chem. Phys.* **132**, 257 (1988).
 [12] A. P. Hitchcock and C. E. Brion, *J. Electron Spectrosc. Relat. Phenom.* **14**, 417 (1978).
 [13] T. Ibuki, N. Takahashi, A. Hiraya, and K. Shobatake, *J. Chem. Phys.* **85**, 5717 (1987).
 [14] L. C. Lee and M. Suto, *Chem. Phys.* **114**, 423 (1987).
 [15] W. Zhang, G. Cooper, T. Ibuki, and C. E. Brion, *Chem. Phys.* **160**, 435 (1992).
 [16] G. R. Burton, W. F. Chan, G. Cooper, and C. E. Brion, *Chem. Phys.* **181**, 147 (1994).
 [17] G. H. Ho, *Chem. Phys.* **226**, 101 (1998).
 [18] M. de Simone, M. Coreno, M. Alagia, R. Richter, and K. C. Prince, *J. Phys. B* **35**, 61 (2002).
 [19] I. H. Suzuki and N. Saito, *Int. J. Mass Spectrom. Ion Processes* **163**, 229 (1997).
 [20] I. H. Suzuki and N. Saito, *Chem. Phys.* **234**, 255 (1998).
 [21] I. H. Suzuki, N. Saito, and J. D. Bozek, *Int. J. Mass Spectrom. Ion Processes* **136**, 55 (1998).
 [22] L. Sheng, F. Qi, H. Gao, Y. Zhang, S. Yu, and W-K. Li, *Int. J. Mass Spectrom. Ion Processes* **161**, 151 (1997).
 [23] J. C. Creasey, D. M. Smith, R. P. Tuckett, K. R. Yoxall, K. Codling, and P. A. Hatherly, *J. Phys. Chem.* **100**, 4350 (1996).
 [24] H. Schenk, H. Oertel, and H. Baumgärtel, *Ber. Bunsenges. Phys. Chem.* **83**, 683 (1979).
 [25] G. C. King and F. H. Read, *J. Phys. B* **12**, 137 (1979).
 [26] A. P. Hitchcock, M. Pocock, and C. E. Brion, *Chem. Phys. Lett.* **49**, 125 (1977).
 [27] K. Ueda, M. Okunishi, H. Chiba, Y. Shimizu, K. Ohmori, Y. Sato, E. Shigemasa, and N. Kosugi, *Chem. Phys. Lett.* **236**, 311 (1995).
 [28] M. N. Piancastelli, *J. Electron Spectrosc. Relat. Phenom.* **100**, 167 (1999).
 [29] J. Berkowitz, in *VUV and Soft X-Ray Photoionization*, edited by U. Becker and D. A. Shirley (Plenum, New York, 1996), p. 263.
 [30] W. C. Stolte, G. Öhrwall, M. M. Sant'Anna, I. Dominguez Lopez, L. T. N. Dang, M. N. Piancastelli, and D. W. Lindle, *J. Phys. B* **35**, L253 (2002).
 [31] W. C. Stolte, M. M. Sant'Anna, G. Öhrwall, I. Dominguez Lopez, M. N. Piancastelli, and D. W. Lindle, *Phys. Rev. A* **68**, 022701 (2003).
 [32] G. Öhrwall, M. M. Sant'Anna, W. C. Stolte, I. Dominguez-

- Lopez, L. T. N. Dang, A. S. Schlachter, and D. W. Lindle, *J. Phys. B* **35**, 4543 (2002).
- [33] W. C. Stolte, D. L. Hansen, M. N. Piancastelli, I. Dominguez Lopez, A. Rizvi, O. Hemmers, H. Wang, A. S. Schlachter, M. S. Lubell, and D. W. Lindle, *Phys. Rev. Lett.* **86**, 4504 (2001).
- [34] S. W. J. Scully, R. A. Mackie, R. Browning, K. F. Dunn, and C. J. Latimer, *J. Phys. B* **35**, 2703 (2002).
- [35] J. A. R. Samson and R. B. Cairns, *Rev. Sci. Instrum.* **36**, 19 (1965).
- [36] E. Hudson, D. A. Shirley, M. Domke, G. Remmers, A. Puschmann, T. Mandel, C. Xue, and G. Kaindl, *Phys. Rev. A* **47**, 361 (1993).
- [37] G. O'Sullivan, *J. Phys. B* **15**, 2385 (1982).
- [38] G. Dujardin, L. Hellner, B. J. Olsson, M. J. Besnard-Ramage, and A. Dadouch, *Phys. Rev. Lett.* **62**, 745 (1989).
- [39] S. W. J. Scully, R. A. Mackie, R. Browning, K. F. Dunn, and C. J. Latimer, *J. Phys. B* **37**, 547 (2004).
- [40] M. B. Robin, *Higher Excited States of Polyatomic Molecules* (Academic, New York, 1974), Vol. I.
- [41] G. C. King and J. W. McConkey, *J. Phys. B* **11**, 1861 (1978).
- [42] J. F. Ying and K. T. Leung, *J. Chem. Phys.* **101**, 7311 (1994).
- [43] L. Pauling, *The Nature of the Chemical Bond* (Cornell University Press, Ithaca, NY, 1963).
- [44] Y. Shimizu, K. Ueda, H. Chiba, M. Okunishi, K. Ohmori, Y. Sato, I. H. Suzuki, T. Ibuki, and K. Okada, *Chem. Phys.* **244**, 439 (1999).